

Non reflection symmetry based polarimetric modeling for forest biophysical characterization using spaceborne PolSAR data

ABHISHEK SOBBANA

March, 2014

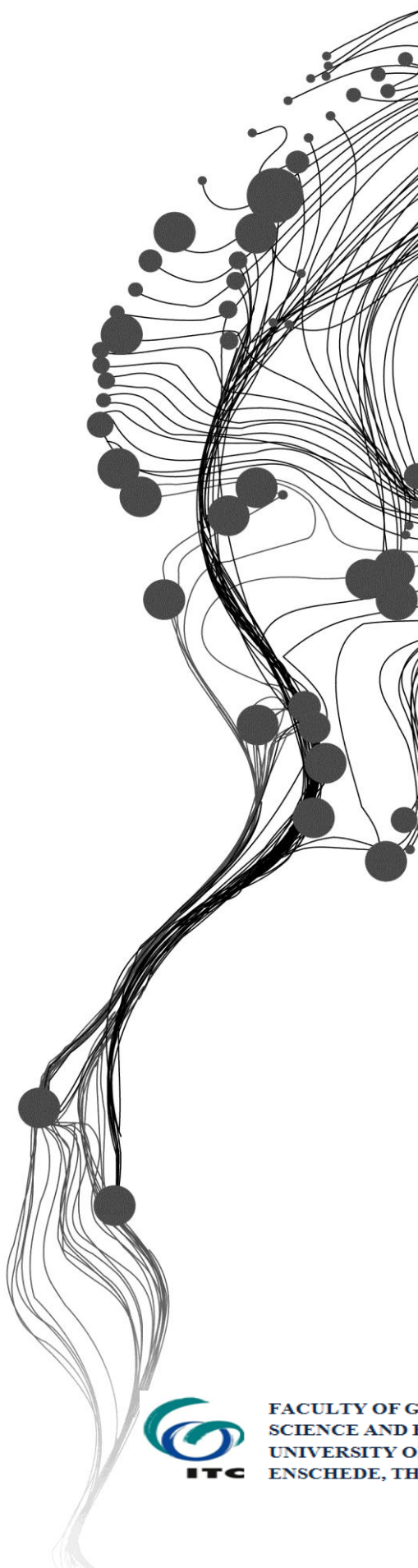
ITC SUPERVISOR

Dr. Wietske Bijker

IIRS SUPERVISORS

Mr. Shashi Kumar,

Dr. SPS Kushwaha



Non reflection symmetry based polarimetric modeling for forest biophysical characterization using spaceborne PolSAR data

ABHISHEK SOBBANA

Enschede, the Netherlands [2014]

Thesis submitted to the Faculty of Geo-information Science and Earth Observation of the University of Twente in partial fulfilment of the requirements for the degree of Master of Science in Geo-information Science and Earth Observation.

Specialization: Geoinformatics

THESIS ASSESSMENT BOARD:

Chairperson (ITC) : Prof. Dr.Ir. A. Stein

External Examiner : Mr. Sanjay (Senior Scientist, DEAL)

ITC Supervisor : Ms. Dr.Ir. Wietske Bijker

IIRS Supervisor : Mr. Shashi Kumar

IIRS Supervisor : Dr. S.P.S Kushwaha

OBSERVERS:

ITC Observer : Dr. Nicholas Hamm

IIRS Observer : Dr. S. K. Srivastav



FACULTY OF GEO-INFORMATION
SCIENCE AND EARTH OBSERVATION,
UNIVERSITY OF TWENTE,
ENSCHEDE, THE NETHERLANDS



INDIAN INSTITUTE OF REMOTE SENSING
Indian Space Research Organisation
Department of Space, Government of India

DISCLAIMER

This document describes work undertaken as part of a programme of study at the Faculty of Geo-information Science and Earth Observation (ITC), University of Twente, The Netherlands. All views and opinions expressed therein remain the sole responsibility of the author, and do not necessarily represent those of the institute.

Dedicated to my parents....

ABSTRACT

Forests comprise of the largest part of vegetation on Earth. Biomass is a measure of carbon dioxide emission, a significant contributor to global warming. The carbon content in the atmosphere can be measured using the stem volume and Above Ground Biomass (AGB). There are various methods to find out the biomass in the environment like in-situ measurements which comes across destructive and non-destructive methods, and also using remote sensing methods. Microwave remote sensing can be used for estimating the biomass and also have a great advantage, since it can penetrate through the canopy because of its longer wavelength. In polarimetric SAR, different polarization channels signifies the information about the target that has been interacting, combination of the entire polarized wave i.e. HH, HV, VH and VV; where HH and VV are called Co-Polarized and HV and VH are called Cross-Polarized channels; gives a potential way to find out the forest biophysical characteristics. RADARSAT-2 has the capability of acquiring all combination of polarized wave. C-band of Radarsat-2 have a wavelength of 5.5cm approximately have been extensively used for estimating biophysical parameter. Traditionally the cross polarized channels are assumed to be identical which signifies the condition of reciprocity. Many Polarimetric decomposition models have been made which consider the property of reciprocity condition. Cloude and Pottier proposed Eigen decomposition technique based on the eigenvalues and eigenvectors of the coherency matrix. The degree of randomness of the scattering process is described by entropy, anisotropy is the complementary of entropy which gives further distinguishable scattering processes and mean alpha angle describes the dominant scattering mechanism. Previous research have shown the potential of coherency matrix, under reciprocity condition, for evaluating the forest biophysical parameters like stem volume and biomass. The polarimetric scattering entropy retrieved from the coherency matrix under reciprocity and non-reciprocity condition were used to investigate relationships with AGB. Regression modelling has been used to estimate biomass by correlating polarimetric entropy and aboveground biomass.

Keywords: *RADARSAT-2, Reciprocity, Entropy, AGB, Eigen decomposition, Polarimetric SAR.*

ACKNOWLEDGEMENTS

At this moment of achievement, I am deeply thankful to my supervisor, Mr. Shashi Kumar Sir, for his constant support and guidance. He was always available with his valuable suggestions whenever I needed his guidance and support throughout my research work. Thank you again, Sir.

I am thankful to my IIRS supervisor, Dr. S.P.S. Kushwaha sir, for his motivation and guidance throughout my research. His guidance has not only helped me in my research but also helped me in improvising myself personally.

I am greatly thankful to my ITC supervisor, Dr. ir. Wietske Bijker madam. Her valuable suggestion and immense knowledge on the subject has helped me in most trying times. Her support and guidance has given me the confidence to approach any subject matter.

I would like to thank Dr. Nicholas Hamm Sir, for his encouragement and initiative to make this course easy and pleasant for me throughout the course period.

I would also like to thank Mr. P.L.N. Raju sir and Dr. S.K. Shrivastav sir for their enduring support and excellent technical infrastructure provided to me for the research work. I thank the CMA department for the technical support extended throughout the course

I am greatly thankful to Dr. Y.V.N. Krishnamurthy sir for providing excellent environment conducive for both research work and recreation.

Last but not the least, my friends also need a special mention here. Raja Raghudeep, Santosh, Praveen, Divya Saranya and Sahithi who has supported everytime when I was going through a very difficult times. I will also thank Ponraj, Raj Bhagat and Kalyani for being their best critique and feedbacks. Special thanks to my juniors Sanjay, Rajasivaranjan, Ramprakash, Aniket, Kiledar, Neeraj and Ashutosh for supporting throughout my project time.

TABLE OF CONTENTS

1. INTRODUCTION	1
1.1. Background.....	1
1.2. Motivation and Problem Statement.....	3
1.3. Research Identification.....	3
1.3.1. Research Objectives.....	3
1.3.2. Research Questions	3
2. LITERATURE REVIEW	4
2.1. SAR Polarimetry.....	4
2.2. Scattering Matrix	5
2.3. Scattering target vector.....	6
2.4. Coherency and Covariance.....	7
2.5. Target decomposition theorem.....	8
2.5.1. Coherent decomposition.....	8
2.5.2. Incoherent decomposition.....	8
2.6. Methods of Estimating Forest Biophysical Parameters	9
3. STUDY AREA	11
3.1. Introduction.....	11
3.2. Significance of the study area	11
4. MATERIALS AND METHODOLOGY	13
4.1. Methodology Flow Chart.....	13
4.2. Dataset Description.....	14
4.3. Data Preprocessing.....	14
4.4. 3×3 Coherency matrix generation.....	15
4.5. 4×4 Coherency matrix generation.....	16
4.6. Eigenvector-Eigenvalue Decomposition.....	16
4.7. Polarimetric scattering Entropy	17
5. RESULTS AND DISCUSSIONS.....	18
5.1. Correlation between the cross polarization.....	18
5.2. Eigenvalue dcomposition and results	19

5.3. Regression Modelling for Biomass Estimation.....	21
5.4. DISCUSSION	23
6. CONCLUSION AND RECOMONDATIONS	26
6.1. Conclusion.....	26
6.2. Recomondations.....	27
REFERENCES	29

LIST OF FIGURES

Figure 2-1: Fundamental behaviour of electromagnetic wave consisting Electric field (E), Magnetic field (M) and Speed of light (c).	4
Figure 2-2: Scattering mechanism (a) Surface Scattering, (b) Double Bounce scattering, and (c) Volume scattering.	6
Figure 3-1: Forest Fire line	11
Figure 3-2: Barkot forest, Rajaji National Park, Study area	12
Figure 4-1: Methodology Flow chart.	13
Figure 4-2: (a) SLC Image and (b) Multilook Image.....	15
Figure 5-1: (a) Backscatter image of HV polarization, (b) Backscatter image of VH polarization, (c) Random points for both HV and VH.....	19
Figure 5-2: Linear regression analysis between HV and VH polarization.	19
Figure 5-3: (a) Entropy image from T3 coherency matrix, (b) Entropy image from T4 coherency matrix	20
Figure 5-4: (a) Entropy for T4 (b) Entropy for T3.....	21
Figure 5-5: Entropy for T3 and T4.....	21
Figure 5-6: Regression analysis between Biomass and Entropy generated from the T3 coherency matrix.....	22
Figure 5-7: Regression Analysis over AGB for measure and estimated (a) Reciprocity (b) Non-Reciprocity	23
Figure 5-8: (a) Entropy under reciprocity, (b) Entropy under non-reciprocity.....	24

1. INTRODUCTION

1.1. Background

Forests comprise of the largest part of vegetation on Earth. Biomass is a measure of carbon dioxide emission, a significant contributor to global warming. RADAR stands for Radio Detection and Ranging; radar remote sensing utilizes the microwave region of wavelength 1mm to 1.3m of the electromagnetic spectrum (EMR) [1]. Extraction of forest physical parameters from the observed scattering of microwaves by surface and volume structure have great deal of interest in polarimetry for radar remote sensing.[2]. Polarization is the orientation of the wave's electric field at a point in space over one period of oscillation. To determine the backscatter coefficients of radar echoes, for any transmit and receive polarizations, polarimetry techniques are used[3]. In synthetic aperture radar (SAR) the method of processing the returned echoes to improve the azimuth resolution allowing the spatial resolution of image scene is used [4].

SAR imaging is a well-developed coherent and microwave remote sensing technique for providing large-scaled two-dimensional (2-D) high spatial resolution images of the Earth's surface reflectivity[5]. In SAR polarimetry, the polarized waves that are transmitted and received have specific polarization. Single polarization transmits horizontal (H) or vertical (V) polarization and receive the corresponding horizontal or vertical. Similarly in dual-polarized SAR there are four components HH, HV transmitted by H and VV, VH transmitted by V, where HH and VV are called co-polarized and HV and VH are called cross polarised, in a fully polarized all the four components are used[5].

Backscatter is the signal received by the sensor from the incident energy coming from the objects on the ground. Backscatter of the radar waves defines the features in the ground based on their dielectric property, surface roughness, water content and incident angle.

Backscattering property of the target object can be described by a scattering matrix, S.

$$S = \begin{bmatrix} S_{HH} & S_{HV} \\ S_{VH} & S_{VV} \end{bmatrix} \quad (1-1)$$

The scattering matrix describes the transformation of electric field of the incident wave to the electric field of the scattered wave [3]. In order to extract physical information about the target, vectorization of scattering matrix is done [6]. In reflection symmetry the cross polarized channels HV and VH are assumed to be identical in the case of space borne SAR systems, for which the Pauli matrix is

$$k = \frac{1}{\sqrt{2}} \begin{bmatrix} S_{HH} + S_{VV} \\ S_{HH} - S_{VV} \\ 2S_{HV} \end{bmatrix} \quad (1-2)$$

The matrix defines three parameters i.e. Surface scattering($S_{HH}+S_{VV}$), Double Bounce scattering($S_{HH}-S_{VV}$) and volume scattering($2S_{HV}$)[2].

The covariance matrix and the coherency matrix, are the second order derivative of scattering matrix, vectorization of scattering matrix is used. In the coherency matrix, the scattering matrix is vectorised by using Pauli based vector [3].

$$T_3 = K \cdot K^{*T} \quad (1-3)$$

Here T_3 is a 3×3 coherency matrix which uses the reflection symmetry polarimetric parameters. To retrieve the amount of scattering information from a coherency matrix a decomposition model such as Freeman and Durden, Yamaguchi, Dong is used [6].

Previous works have focused on reflection symmetry based polarimetry for the retrieval of forest biophysical characteristics. The current research focuses on retrieving these parameters using non-reflection based polarimetry. The cross-pol channels in non reflection symmetry based polarimetry are not assumed to be identical. Yamaguchi et al [7] have focused their research on a scattering model that decomposes the elements of a coherency matrix using four components (single bounce, double bounce, volume scattering and helix). Their method of decomposition takes into consideration the non reflection symmetry based concepts of polarimetry. The central concept of Chen et al.'s [8] research was to reduce the over estimation of volume scattering due to orientation angle shift. It is difficult to synthesize the orientation angle to zero in reflection symmetry but is not the case in non reflection symmetry as orientation angle shift is not a major concern in non reflection symmetry based polarimetry. The current research focuses on the retrieval of forest biophysical characteristics using non reflection symmetry based polarimetry.

1.2. Motivation and Problem Statement

Previous works have focused on reflection symmetry based polarimetry for the retrieval of forest biophysical characteristics. The current research focuses on retrieving these parameters using non-reflection based polarimetry. The cross-pol channels, in non reflection symmetry based polarimetry, are not assumed to be identical. The coherency matrix is a second order derivative of scattering matrix where all possible scattering information can be retrieved. Cloude and Pottier has proposed Eigen decomposition providing physical information, but for simplification three secondary parameters are derived from the eigenvector and eigenvalue functions, i.e. entropy (H), anisotropy (A) and mean alpha angle (α) [9]. The current research focuses on the retrieval of forest biophysical characteristics using non reflection symmetry based polarimetry.

1.3. Research Identification

1.3.1. Research Objectives

To retrieve scattering information contributed by forest vegetation and modelling for biophysical characterization using concept of non-reflection symmetry in PolSAR data.

Sub-objectives:

- To generate decomposition model for 4×4 coherency matrix.
- To retrieve the scattering elements from both 3×3 coherency matrix and 4×4 coherency matrix.
- To derive scattering parameters which will be used for estimating forest biophysical parameter.
- Test the feasibility of non-reflection symmetry based polarimetric technique for retrieval of forest characteristics

1.3.2. Research Questions

To reach the above objective the following questions need to be answered.

1. Which technique can decompose a 4×4 coherency matrix?
2. Which scattering parameters will be needed for biomass estimation?
3. To what degree are non reflection symmetry based polarimetry parameters different from reflection symmetry based parameters?
4. Can non reflection symmetry be used for retrieval of forest biophysical characteristics?
5. How viable is the non reflection symmetry based polarimetry technique for estimating forest biophysical parameters in comparison to the results obtained by the field data?

2. LITERATURE REVIEW

2.1. SAR Polarimetry

Radar stands for Radio Detection and Ranging. The principle behind radar is it will measure the distance to an object by transmitting electromagnetic signal and receive the reflected signal from the object. Electromagnetic waves propagates at speed of light, if one can measure the propagation time(t) from sensor to object and also its echo, then it is easily to calculate the range(R) as

$$R = \frac{1}{2}ct \quad (2-1)$$

C is speed of light in vacuum. A radar system transmits radar signals of known wavelength, amplitude, phase and polarization. Figure 2-1 shows the three components in electromagnetic wave i.e. electric field(E), magnetic field(M) and speed of light(C), where electric and magnetic field are orthogonal to each other which are described by Maxwell's equations[10].

Polarization describes the regularity of electric and magnetic field component of the electromagnetic wave. In polarization, electric field has two components horizontal and vertical, combining these two components yields a net electric field vector [11].

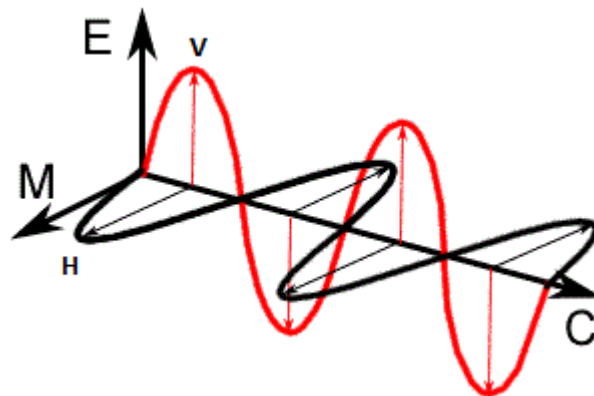


Figure 2-1: Fundamental behaviour of electromagnetic wave consisting Electric field (E), Magnetic field (M) and Speed of light (c).

Radar transmit microwave radiation according to which it is designed to transmit either horizontal (H) or vertical (V) polarized. A Radar polarimetry is the analysis of these transmitted polarized wave and its combination[12].

Using these radars there can be four combination of polarization which transmit and receives the polarized wave.

- ➔ HH - Horizontal transmit and horizontal receive
- ➔ VV - Vertical transmit and vertical receive
- ➔ HV - Horizontal transmit and vertical receive
- ➔ VH - Vertical transmit and horizontal receive

HH and VV are referred as like-polarized or co-polarized since they transmit and receive polarization of the same. HV and VH are called as cross-polarized since they transmit and receive polarization of opposite to one another. In a fully polarimetric all the four components are used[9]. Synthetic Aperture Radar (SAR) polarimetric acquires four images each one of the component i.e. HH, VV, HV, and VH. The information in SAR polarimetry can consist about frequency, intensity or polarization of the electromagnetic wave. The interaction between the surface, the electromagnetic waves and the atmosphere depends on the frequency of the waves. Based on their transmission a SAR system can have single polarized consisting HH or HV or VH or VV, dual polarized i.e. HH and VV or HH and HV or VV and VH, and quad polarized transmit and receive all polarization [4][10].

2.2. Scattering Matrix

When a target is being interacted with any polarized wave (either horizontal or vertical) the scattered wave from the target can have both horizontal and vertical polarized wave. A scattering matrix, S , describes the backscattering property of the target which will have a complete basis set of electromagnetic wave.

$$\begin{bmatrix} E_h^S \\ E_v^S \end{bmatrix} = \begin{bmatrix} S_{hh} & S_{hv} \\ S_{vh} & S_{vv} \end{bmatrix} \begin{bmatrix} E_h^i \\ E_v^i \end{bmatrix} \quad (2-2)$$

Where E^S and E^i are electric field of scattered wave and incident wave respectively. Since the elements in the scattering matrix are complex they are measured by magnitude and phase from its corresponding channel in the radar system[13], [14].

The scattering response from the target depend upon the geometry and reflectivity property of the target. Surface scattering is modelled when surface is meant to be rough or plane, Double bounce is modelled when the polarized wave is reflected from orthogonal surface, and Volume scattering is defined when the polarized wave are completely scattered a canopy layer (Figure 2-2) [1].

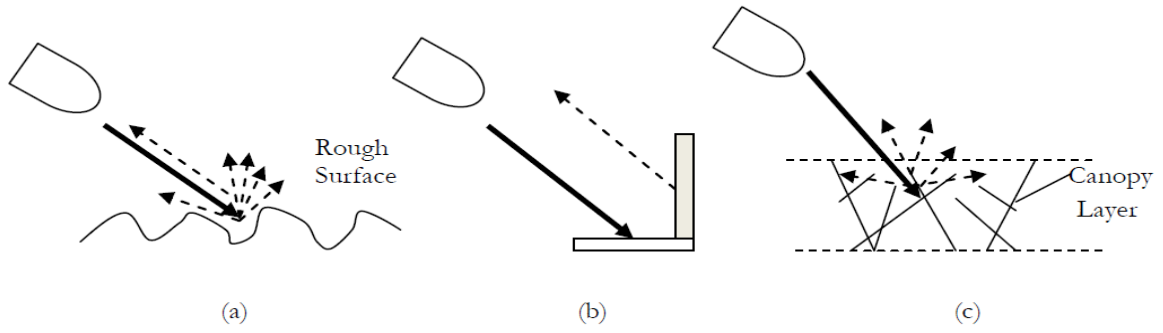


Figure 2-2: Scattering mechanism (a) Surface Scattering, (b) Double Bounce scattering, and (c) Volume scattering.

Using Polarimetric SAR (PolSAR) it becomes easier to extract all the possible scattering information from single SAR resolution cell. The scattering information can be derived using PolSAR decomposition model.

2.3. Scattering target vector

In order to extract physical information of the target, vectorization of scattering matrix is done, which yields to a target vector [6]. In polarimetric radar literature there are two bases which favor in the vectorization of scattering matrix which are, Lexicographic basis (ψ_L) and Pauli spin matrix set (ψ_P)[9][15].

A complex Pauli spin matrix basis set is given by

$$\{\psi_P\} = \left\{ \sqrt{2} \begin{bmatrix} 1 & 0 \\ 0 & 1 \end{bmatrix}, \sqrt{2} \begin{bmatrix} 1 & 0 \\ 0 & -1 \end{bmatrix}, \sqrt{2} \begin{bmatrix} 0 & 1 \\ 1 & 0 \end{bmatrix}, \sqrt{2} \begin{bmatrix} 0 & -j \\ j & 0 \end{bmatrix} \right\} \quad (2-3)$$

Its corresponding pauli feature vector k is,

$$k = \frac{1}{\sqrt{2}} \begin{bmatrix} S_{HH} + S_{VV} \\ S_{HH} - S_{VV} \\ S_{HV} + S_{VH} \\ j(S_{HV} - S_{VH}) \end{bmatrix} \quad (2-4)$$

The second basis is the lexicographic matrix basis set (ψ_L) which is given by

$$\{\psi_L\} = \left\{ 2 \begin{bmatrix} 1 & 0 \\ 0 & 0 \end{bmatrix}, 2 \begin{bmatrix} 0 & 1 \\ 0 & 0 \end{bmatrix}, 2 \begin{bmatrix} 0 & 0 \\ 1 & 0 \end{bmatrix}, 2 \begin{bmatrix} 0 & 0 \\ 0 & 1 \end{bmatrix} \right\} \quad (2-5)$$

Its corresponding lexicographic feature vector Ω is,

$$\Omega = \begin{bmatrix} S_{HH} \\ S_{HV} \\ S_{VH} \\ S_{VV} \end{bmatrix} \quad (2-6)$$

2.4. Coherency and Covariance

In a dynamically changing environment many targets situated are dependent on the temporal and spatial variations, with which many scatters are comparable with partially polarized waves. For which, a second order moments can be extracted from coherency(T) and covariance(C) matrix which will evolve the different scatters which are involved in the radar targets[9].

The second order moment of a matrix is derived by multiplying the first order feature vector to its complex conjugate.

$$T = \langle k \cdot k^{*T} \rangle \quad \text{and} \quad C = \langle \Omega \cdot \Omega^{*T} \rangle$$

Traditionally the concepts of reciprocity have been used in second order derivative of scattering matrix. In reciprocity, the cross polarized channels are assumed to be identical or symmetrical i.e. $S_{HV} = S_{VH}$ [1], [9], [16]–[18]. Under this assumption the second order moment of the scattering matrix will be a 3×3 matrix given as,

$$[T_3] = \langle k \cdot k^{*T} \rangle = \frac{1}{2} \begin{bmatrix} S_{HH} + S_{VV} \\ S_{HH} - S_{VV} \\ 2S_{HV} \end{bmatrix} \times \begin{bmatrix} S_{HH} + S_{VV} & S_{HH} - S_{VV} & 2S_{HV} \end{bmatrix} \quad (2-7)$$

$$[T_3] = \frac{1}{2} \begin{bmatrix} \langle |S_{HH} + S_{VV}|^2 \rangle & \langle (S_{HH} + S_{VV})(S_{HH} - S_{VV})^* \rangle & \langle 2(S_{HH} + S_{VV})S_{HV}^* \rangle \\ \langle (S_{HH} - S_{VV})(S_{HH} + S_{VV})^* \rangle & \langle |S_{HH} - S_{VV}|^2 \rangle & \langle 2(S_{HH} - S_{VV})S_{HV}^* \rangle \\ \langle 2S_{HV}(S_{HH} + S_{VV})^* \rangle & \langle 2S_{HV}(S_{HH} - S_{VV})^* \rangle & \langle 4|S_{HV}|^2 \rangle \end{bmatrix} \quad (2-8)$$

and

$$[C_3] = \begin{bmatrix} S_{HH} \\ \sqrt{2}S_{HV} \\ S_{VV} \end{bmatrix} \times \begin{bmatrix} S_{HH} & \sqrt{2}S_{HV} & S_{VV} \end{bmatrix} \quad (2-9)$$

$$[C_3] = \begin{bmatrix} \langle |S_{HH}|^2 \rangle & \sqrt{2}\langle S_{HH}S_{HV}^* \rangle & \langle S_{HH}S_{VV}^* \rangle \\ \sqrt{2}\langle S_{HV}S_{HH}^* \rangle & 2\langle |S_{HV}|^2 \rangle & \sqrt{2}\langle S_{HV}S_{VV}^* \rangle \\ \langle S_{VV}S_{HH}^* \rangle & \sqrt{2}\langle S_{VV}S_{HV}^* \rangle & \langle |S_{HH}|^2 \rangle \end{bmatrix} \quad (2-10)$$

This research consider the concepts of non-reciprocity, where the cross polarized channels are supposed to be not identical i.e. $S_{HV} \neq S_{VH}$. Using this the second order moment of scattering matrix will be a 4×4 matrix given by,

$$[T_4] = \langle k \cdot k^{*T} \rangle = \frac{1}{2} \begin{bmatrix} \langle |S_{HH} + S_{VV}|^2 \rangle & \langle (S_{HH} + S_{VV})(S_{HH} - S_{VV})^* \rangle & \langle (S_{HH} + S_{VV})(S_{HV} + S_{VH})^* \rangle & \langle -j(S_{HH} + S_{VV})(S_{HV} - S_{VH})^* \rangle \\ \langle (S_{HH} - S_{VV})(S_{HH} + S_{VV})^* \rangle & \langle |S_{HH} - S_{VV}|^2 \rangle & \langle (S_{HH} - S_{VV})(S_{HV} + S_{VH})^* \rangle & \langle -j(S_{HH} - S_{VV})(S_{HV} - S_{VH})^* \rangle \\ \langle (S_{HV} + S_{VH})(S_{HH} + S_{VV})^* \rangle & \langle (S_{HV} + S_{VH})(S_{HH} - S_{VV})^* \rangle & \langle |S_{HV} + S_{VH}|^2 \rangle & \langle -j(S_{HV} + S_{VH})(S_{HV} - S_{VH})^* \rangle \\ \langle j(S_{HV} - S_{VH})(S_{HH} + S_{VV})^* \rangle & \langle j(S_{HV} - S_{VH})(S_{HH} - S_{VV})^* \rangle & \langle j(S_{HV} - S_{VH})(S_{HV} + S_{VH})^* \rangle & \langle |S_{HV} - S_{VH}|^2 \rangle \end{bmatrix} \quad (2-11)$$

and

$$[C_4] = \langle \Omega \cdot \Omega^{*T} \rangle = \frac{1}{2} \begin{bmatrix} \langle |S_{HH}|^2 \rangle & \langle S_{HH}S_{HV}^* \rangle & \langle S_{HH}S_{VH}^* \rangle & \langle S_{HH}S_{VV}^* \rangle \\ \langle S_{HV}S_{HH}^* \rangle & \langle |S_{HV}|^2 \rangle & \langle S_{HV}S_{VH}^* \rangle & \langle S_{HV}S_{VV}^* \rangle \\ \langle S_{VH}S_{HH}^* \rangle & \langle S_{VH}S_{HV}^* \rangle & \langle |S_{VH}|^2 \rangle & \langle S_{VH}S_{VV}^* \rangle \\ \langle S_{VV}S_{HH}^* \rangle & \langle S_{VV}S_{HV}^* \rangle & \langle S_{VV}S_{VH}^* \rangle & \langle |S_{VV}|^2 \rangle \end{bmatrix} \quad (2-12)$$

2.5. Target decomposition theorem

In order to determine various scattering mechanism which are involved by the scattering matrix, target decomposition theorems are applied. The decomposition techniques were basically comes under two group's i.e. coherent and incoherent target decomposition.

2.5.1. Coherent decomposition

The scattering information from coherent decomposition are derived from the understanding of the scattering matrix. Many known coherent target decomposition theorems which were proposed by Pauli, Cameron and Krogager. Pauli decomposition theorem decomposed the scattering matrix into three scattering mechanism under reciprocity condition: Surface scattering (Single or Odd bounce), Double bounce scattering (Even bounce scattering), Volume scattering.

Krogager in [19] developed a decomposition which decomposes the scattering matrix into three coherent components having physical interpretation in terms of sphere, diplane and helix target under a change of orientation angle. The decomposition method takes the scattering matrix of the target and then transformed by a rotation operator, due to orientation of the target towards the antenna is not always aligned, and decompose into three scattering mechanism.

2.5.2. Incoherent decomposition

Incoherent decomposition decomposes second order derivative matrices i.e. coherency matrix and covariance matrix for describing the complex scattering behaviour of the targets. Significant incoherent decomposition was proposed by Freeman and Durden and Yamaguchi.

Freeman and Durden in [16] proposed a three component scattering model for polarimetric SAR data, with the assumptions of reciprocity, the second order derivative scattering matrix is decomposed into three components. Using three scattering mechanism, first the Bragg scatter from

rough surface; second the double bounce from orthogonal surface having different dielectric constant; and canopy scatter from cloud of randomly oriented dipoles, the decomposition will make to discriminate between dense and sparse forest, scattering mechanism. The model-fitting approach on polarimetric SAR data works well without the ground truth data.

Yamaguchi *et al.*, in [20][21][22][23] proposed a four component decomposition model which uses both 3×3 coherency matrix and 3×3 covariance matrix which deals with the assumption of non-reciprocity case. The decomposition model is an extension to Freeman and Durden decomposition model in this he involved another scattering element Helix which was introduced by Krogager. Yamaguchi *et al.*, in [20] also gave their contribution towards volume scattering matrix in the four decomposition model according to the magnitude of the backscattering. Volume scattering is dominant to vegetated areas due to its vertical structure, for which a new probability distribution is applied to the covariance matrix and two covariance matrices from horizontal and vertical scatters are averaged. According to which Yamaguchi proposed appropriate volume scattering covariance matrix according to the magnitude difference.

Cloude and Pottier in [24] proposed a decomposition technique based on the eigenvalues and eigenvectors of the coherency matrix. Different scatter process is described by the eigenvector analysis and their relative magnitude information is obtained by eigenvalue analysis [25]. The concepts was evolved to scattering matrix parameter of the target by employing three level Bernoulli statistical model [9]. This method was based on the eigenvalue analysis of the 3×3 coherency matrix [24]. The eigen decomposition analysis provides physical information, but for simplification three secondary parameters are derived from the eigenvector and eigenvalue functions, i.e. entropy (H), anisotropy (A) and mean alpha angle (α) [9]. The degree of randomness of the scattering process is described by entropy, anisotropy is the complementary of entropy which gives further distinguishable scattering processes and mean alpha angle describes the dominant scattering mechanism [11]. Using eigen decomposition many classifications techniques were also developed to identify man made structure [26], [27] and forest parameters [28].

2.6. Methods of Estimating Forest Biophysical Parameters

Biomass is a measure of carbon dioxide emission, a significant contributor to global warming. Biomass can be measured using different techniques like in-situ measurements, which comes again with destructive and non-destructive methods of estimating, and estimating by remote sensing data.

Destructive methods of estimating biomass deals with harvesting the vegetation like trees, trunks and stem. The harvested materials are then dried up and then biomass is calculated, these kind of methods cannot be used for regular use, but the intension of the destructive method is to calculate the biomass for different kind of species.

Non-destructive methods of estimating the biomass deals with the characteristics of the tree like height of the tree, Diameter at Breast Height (DBH), and basal area. These components are used in empirical formulas to estimate the biomass. Non-destructive methods are time consuming when it comes to a dense forest but still is better than the destructive methods.

Apart from the in-situ measurements, many conventional methods and approaches are derived to retrieve the biomass using remote sensing data. A semi-empirical model was developed by Attema et al. in [29], water cloud model (WCM) which will model the backscatter from the canopy. The model considers only the interaction of surface and the canopy; it does not consider the scattering came from the canopy gaps [29].

Santoro et al. [30] developed interferometric WCM which is similar to the WCM which uses the coherence generated from multi-temporal interferometric SAR data and then stem volume is retrieved [30]. Another contribution by Santoro was retrieval of stem volume from JERS-1 HH polarization for which he used the inversion of WCM to include radar backscatter from the canopy gaps[31].

Mette et al. [32] have estimated the biomass and height using polarimetric interferometric SAR data in L-band. Mette used a model inversion technique on Random Volume Over Ground (RVOG). Using the estimated height, biomass is retrieved using the height-biomass allometric equation [32]. Regression modelling in [33]–[39] has also been used to estimate biomass by correlating Radar backscatter coefficient and biophysical parameter, like aboveground biomass, stem volume and basal area. Hoekman et al. [33] have worked with AirSAR C-, L- and P-band data, in which comparison between the backscatter of C-, L-, and P-band to the onsite Biomass measurement. A quantitative analysis by Hoekman showed there is a good correlation between the L- and P-band with the above ground biomass up to ~200 tons/ha. Dobson in [34] showed Regression analysis which was carried out between the backscattering values and aboveground biomass. The backscatter coefficient (σ°), retrieved from sample plots at HH, VV, VH and HV were used to investigate relationships with aboveground tree biomass. Highest sensitivity of the biomass was shown by the polarization which are more sensitive to specular scattering mechanism from the trunk and the ground surface, i.e. HH and HV. The linear regression analysis showed the biomass have a saturation point upon the backscatter, depending on the wavelength i.e. P- and L-band, with a region of 100-200 tons/ha.

3. STUDY AREA

3.1. Introduction

The study area, Barkot forest, is located in the valley next to the foothills of the Himalayas in India and is located at around 40 km away from Dehradun city. The study area lies between 30.03° - 30.16° N latitude and 78.07° - 78.19° E longitude.

3.2. Significance of the study area

The area is known as Barkot and has a relatively flat terrain which does not require the use of external Digital Elevation Model (DEM). The elevation range of the Barkot forest ranges from 300 to 600m. The Barkot Forest area has also been chosen as it is dominated by Sal (*Shorea robusta*) forests and its dense canopy makes it useful for studying volume scattering. The ground stem interactions (double bounce) that take place within the vegetative layer can also be observed making this particular area viable for studying the various scattering mechanisms that take place within a forest. Figure 3-1 shows the Fire line which is generally a strip of cleared land used for to arrest the advance of a fire. The climate of the area is moderate because the area is at the foothills of the Himalayas.

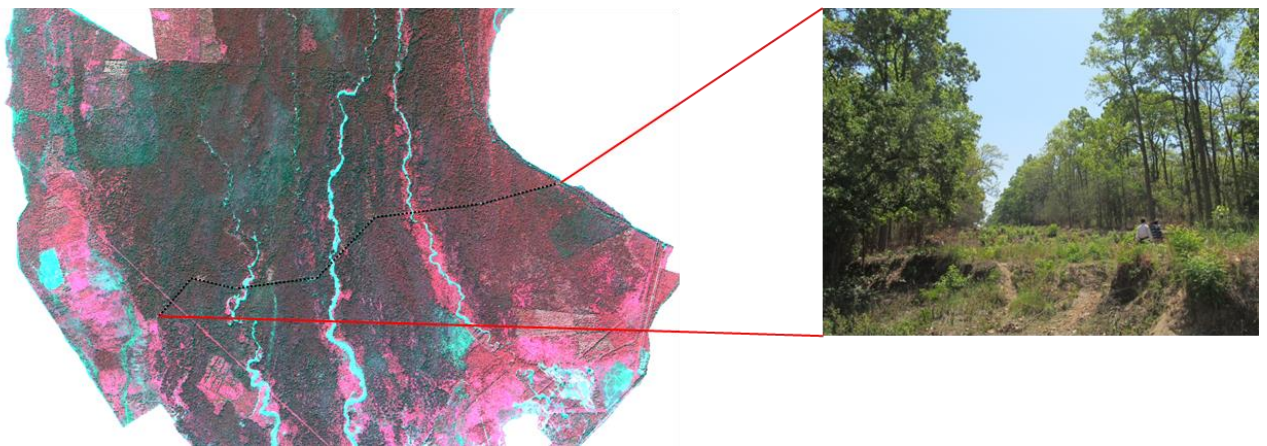


Figure 3-1: Forest Fire line

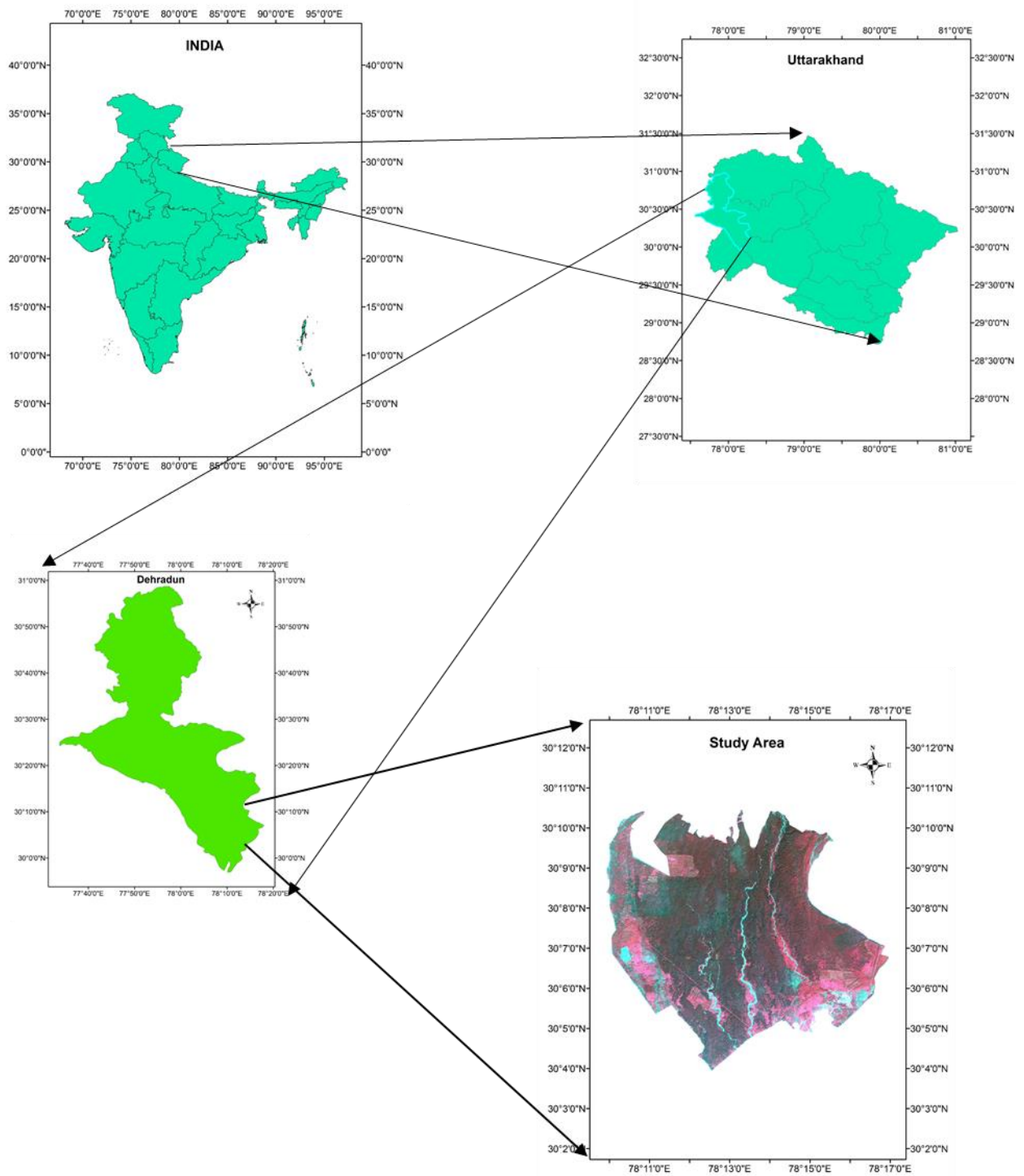


Figure 3-2: Barkot forest, Rajaji National Park, Study area (Source: IRS ResourceSat-2 sensor 14 October 2012)

4. MATERIALS AND METHODOLOGY

4.1. Methodology Flow Chart

The Figure 4-1 shows the methodology used in present study.

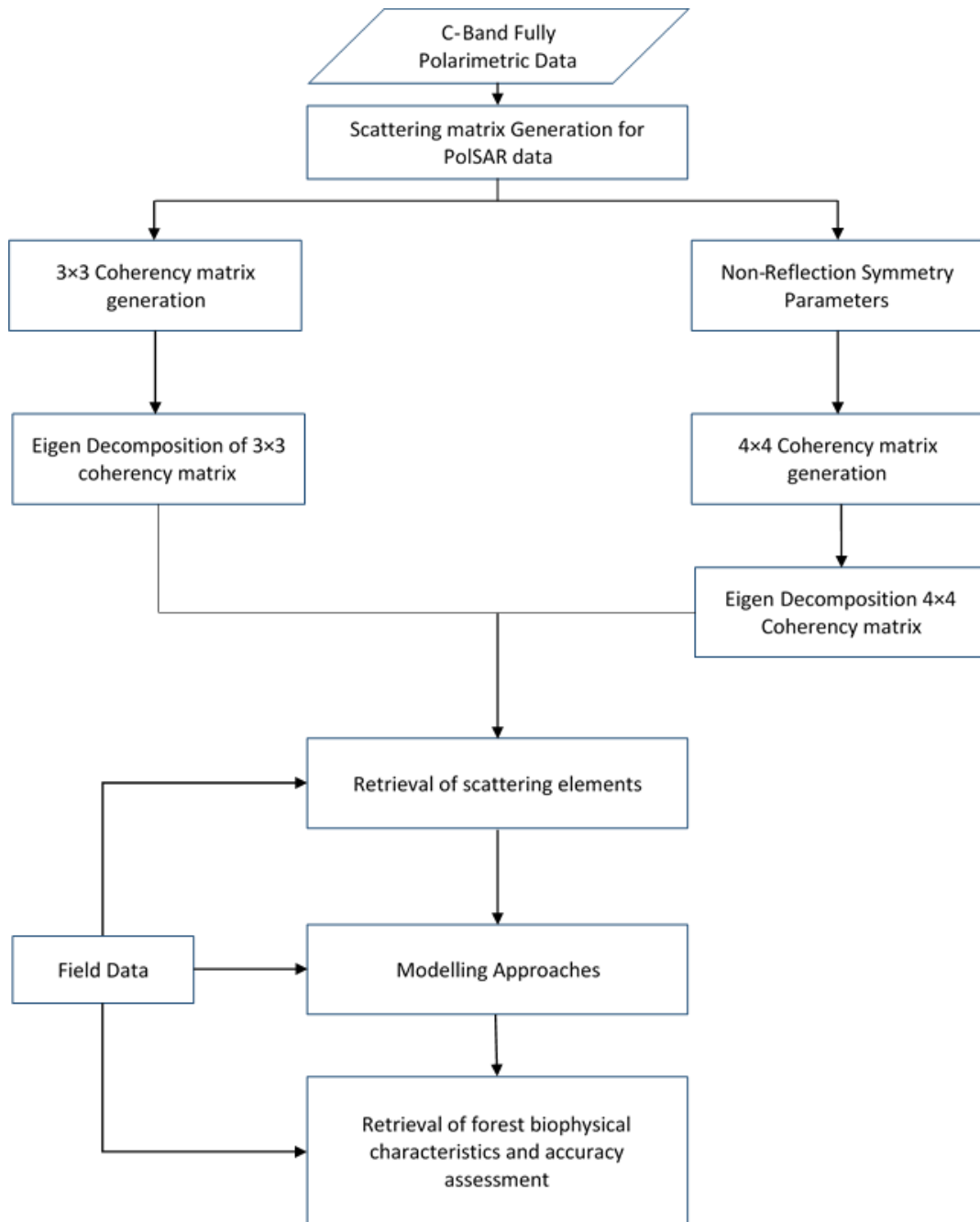


Figure 4-1: Methodology Flow chart.

4.2. Dataset Description

The data used in current study is of RADARSAT-2 in C-band. RADARSAT-2 is an earth observation satellite launched by Canadian Space Agency (CSA). The radarsat-2 data is provided by SOAR (Science and Operational Applications Research for Radarsat-2) program, for research and testing purposes, which is a joint program between MacDonald Dettwiler and Associates Ltd. and Canadian government through the CSA and Natural Resources Canada's centre for remote sensing (CCRS) [40]. The satellite has a multiple polarization modes which includes a fully polarimetric mode in which a Quad (HH, HV, VH and VV) polarized data are retrieved [41]. The description of the dataset is given in table 4-1.

Table 4-1: Data characteristics.

Sensor	RADARSAT-2
Acquisition date	04-Mar-2013 00:44:48
Wavelength	5.6cm
Polarisation	HH+HV+VV+VH
Orbit direction	Descending
Orbit Number	27246
Incidence Angle	40°
Centre Latitude	30.1709
Centre Longitude	78.1865

4.3. Data Preprocessing

The data acquired from radarsat-2 is in quad-polarization (HH, HV, VH and VV) having C-band data. The acquired radar data is projected in slant range geometry, which is the datasets are in SLC (Single look Complex) format, generally described by two spatial resolutions projected in a SAR system, i.e. Azimuth resolution and Range resolution. The resolution measured along the flight path is azimuth whereas the complimentary measurement is described by range resolution. Due to the slant range geometry of radar data, distortions can be observed in the images, where the objects appearing under near range will look like compressed compared to the object that are in far range. To overcome the distortion, the slat range geometry is converted to ground range plane, this process is called as Multilooking. Figure 4-2 shows the multilooked image of SLC format data of the study area.

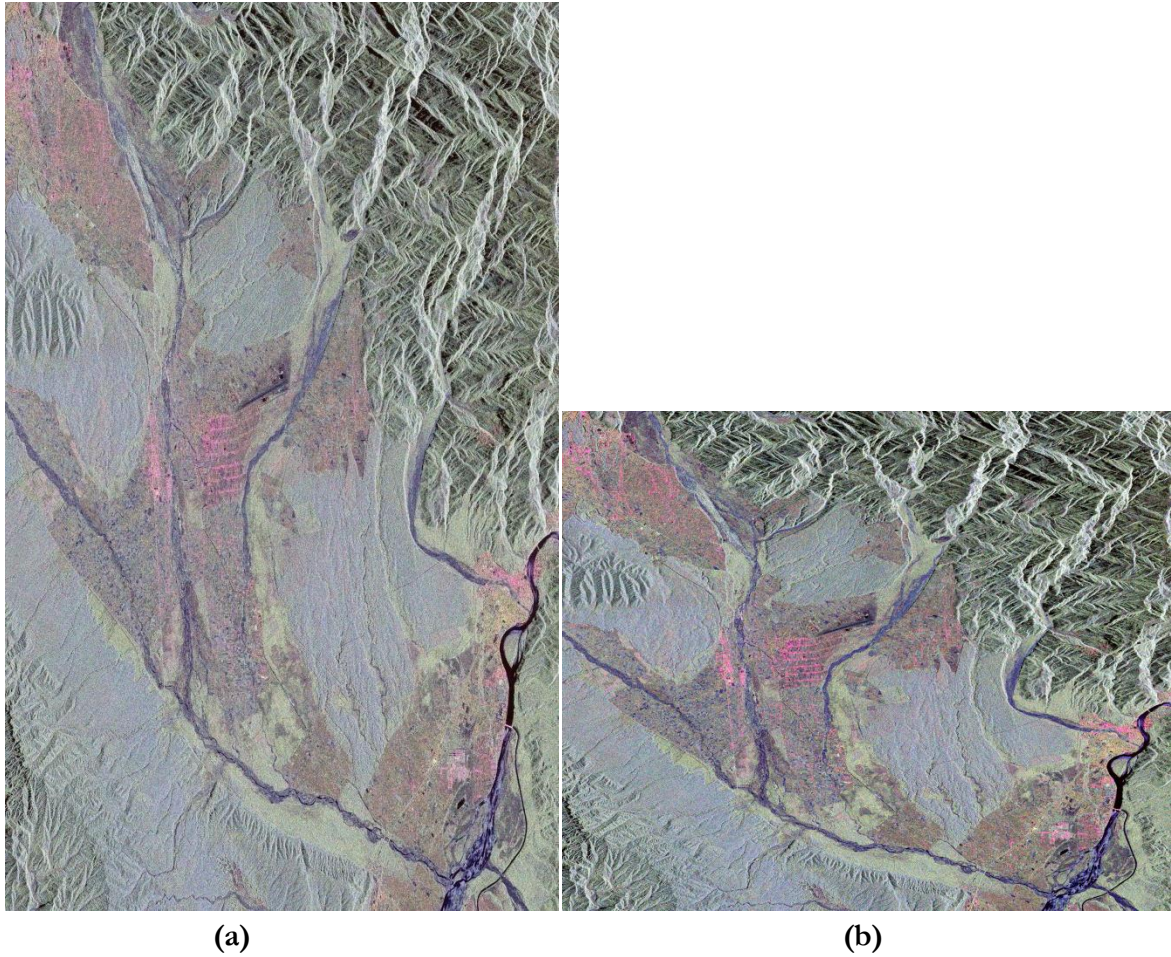


Figure 4-2: (a) SLC Image and (b) Multilook Image.

4.4. 3×3 Coherency matrix generation

Under the condition of reciprocity, the Pauli matrix into its complex conjugate transpose. When the cross polarized channels are assumed to be identical, a T3 coherency matrix is generated. This coherency matrix is retrieved by multiplying

$$K = \frac{1}{\sqrt{2}} \begin{bmatrix} S_{HH} + S_{VV} \\ S_{HH} - S_{VV} \\ 2S_{HV} \end{bmatrix} \quad (4.1)$$

$$T_3 = K \cdot K^{*T} \quad (4.2)$$

$$T_3 = \frac{1}{2} \begin{bmatrix} \langle |S_{HH} + S_{VV}|^2 \rangle & \langle (S_{HH} + S_{VV})(S_{HH} - S_{VV})^* \rangle & \langle 2(S_{HH} + S_{VV})S_{HV}^* \rangle \\ \langle (S_{HH} - S_{VV})(S_{HH} + S_{VV})^* \rangle & \langle |S_{HH} - S_{VV}|^2 \rangle & \langle 2(S_{HH} - S_{VV})S_{HV}^* \rangle \\ \langle 2S_{HV}(S_{HH} + S_{VV})^* \rangle & \langle 2S_{HV}(S_{HH} - S_{VV})^* \rangle & \langle 4|S_{HV}|^2 \rangle \end{bmatrix} \quad (4.3)$$

Where $\langle \rangle$ represents the ensemble averaging in the data processing, the superscripts $*$ represents the complex conjugate and t represents the transpose.

4.5. 4×4 Coherency matrix generation

Under the condition of non-reciprocity, we consider the cross-pol channels meant not to be identical, i.e. $HV \neq VH$. Based on that the linear combination of Pauli matrix will arise a 4×4 coherency matrix.

Using the first group of complex Pauli spin matrix basis set $\{\psi_P\}$, the Pauli feature vector is given by,

$$K = \frac{1}{\sqrt{2}} \begin{bmatrix} S_{HH} + S_{VV} \\ S_{HH} - S_{VV} \\ S_{HV} + S_{VH} \\ j(S_{HV} - S_{VH}) \end{bmatrix} \quad (4.4)$$

The coherency matrix (T_4) is generated from the product of Pauli target vector with its conjugate transpose, which is given by,

$$T_4 = K \cdot K^{*T} \quad (4.4)$$

$$T_4 = \frac{1}{2} \begin{bmatrix} \langle |S_{HH} + S_{VV}|^2 \rangle & \langle (S_{HH} + S_{VV})(S_{HH} - S_{VV})^* \rangle & \langle (S_{HH} + S_{VV})(S_{HV} + S_{VH})^* \rangle & \langle -j(S_{HH} + S_{VV})(S_{HV} - S_{VH})^* \rangle \\ \langle (S_{HH} - S_{VV})(S_{HH} + S_{VV})^* \rangle & \langle |S_{HH} - S_{VV}|^2 \rangle & \langle (S_{HH} - S_{VV})(S_{HV} + S_{VH})^* \rangle & \langle -j(S_{HH} - S_{VV})(S_{HV} - S_{VH})^* \rangle \\ \langle (S_{HV} + S_{VH})(S_{HH} + S_{VV})^* \rangle & \langle (S_{HV} + S_{VH})(S_{HH} - S_{VV})^* \rangle & \langle |S_{HV} + S_{VH}|^2 \rangle & \langle -j(S_{HV} + S_{VH})(S_{HV} - S_{VH})^* \rangle \\ \langle j(S_{HV} - S_{VH})(S_{HH} + S_{VV})^* \rangle & \langle j(S_{HV} - S_{VH})(S_{HH} - S_{VV})^* \rangle & \langle j(S_{HV} - S_{VH})(S_{HV} + S_{VH})^* \rangle & \langle |S_{HV} - S_{VH}|^2 \rangle \end{bmatrix}$$

4.6. Eigenvector-Eigenvalue Decomposition

Based on Eigen decomposition of coherency matrix ($[T]$), Eigen vector and Eigen value based decomposition was proposed by Cloudie and Pottier.

According to the Eigen decomposition, the coherency matrix $\langle [T_3] \rangle$ can be written as

$$T_i = [U_i] \times [\Sigma_i] \times [U_i]^T \quad (4.5)$$

Where i represent the dimension of the polarimetry, i.e. 3 under reciprocity condition and 4 under non-reciprocity condition, $[\Sigma_i]$ represents the Eigen value and $[U_i]$ represents Eigen vector of the coherency matrix $\langle [T_i] \rangle$ and is given by1

$$[\Sigma_3] = \begin{bmatrix} \lambda_1 & 0 & 0 \\ 0 & \lambda_2 & 0 \\ 0 & 0 & \lambda_3 \end{bmatrix} \quad \& \quad \Sigma_4 = \begin{bmatrix} \lambda_1 & 0 & 0 & 0 \\ 0 & \lambda_2 & 0 & 0 \\ 0 & 0 & \lambda_3 & 0 \\ 0 & 0 & 0 & \lambda_4 \end{bmatrix}$$

$$[U_3] = [U_1 \quad U_2 \quad U_3] \quad \& \quad U_4 = [U_1 \quad U_2 \quad U_3 \quad U_4]$$

Based on second order statistics Cloude and Pottier proposed a method for extracting average parameters.

4.7. Polarimetric scattering Entropy

The polarimetric scattering entropy describes the global measure of scattering process, describing the distribution of scattering components. The degree of randomness of the scattering process is described by Entropy. The polarimetry entropy provides an efficient parameter describing each scatter type within ensemble, which is given by

$$H = -\sum_{k=1}^N P_k \log_N(P_k) \quad (4.6)$$

Where, N is the dimension of the polarimetry, P_k is the pseudo-probabilities which is retrieved from the eigenvalues λ_i which is given by

$$P_k = \frac{\lambda_i}{\sum_{i=1}^N \lambda_i} = \frac{\lambda_i}{SPAN} \quad (4.7)$$

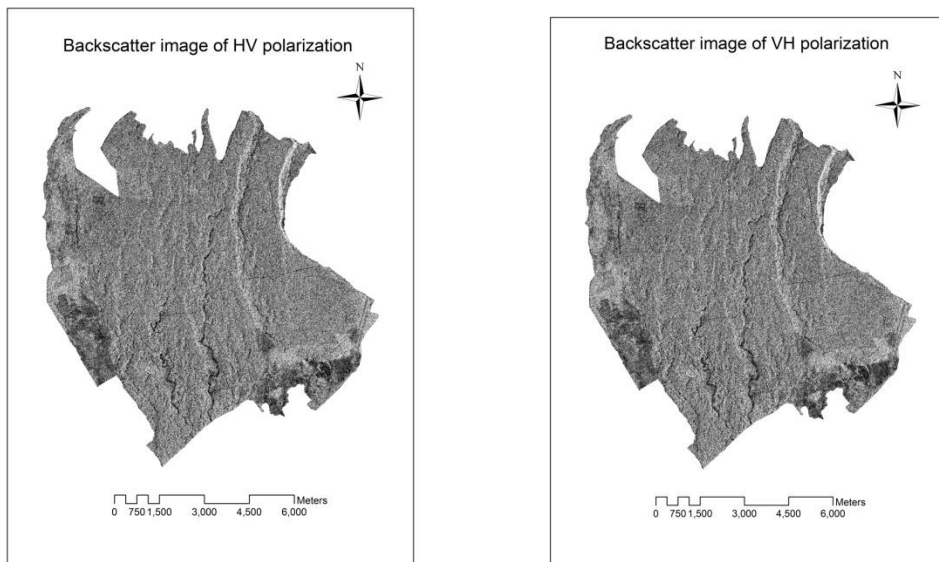
The entropy H is defined by Eigen values of the coherency matrix. It is a significant feature because it consider both the physical parameter, like biomass and canopy configuration, and also the randomness of the scattering media[42].

Coherency matrix under non reciprocity condition is 4×4 positive hermitian matrix having real non-negative eigenvalues [24]. The polarimetric scattering process of the terrain is shown by the amplitude and the difference of the four eigenvalues which are functionally associated to each other. The polarimetric scattering entropy generally varies from 0 to 1, if the $H < 0.3$ then the system is considered as dominant scattering mechanism which describes that the point target is specifically identifiable. If the entropy is high, i.e. $H=1$, then the system is considered as a noise since it doesn't have a single equivalent point scatter [43].

5. RESULTS AND DISCUSSIONS

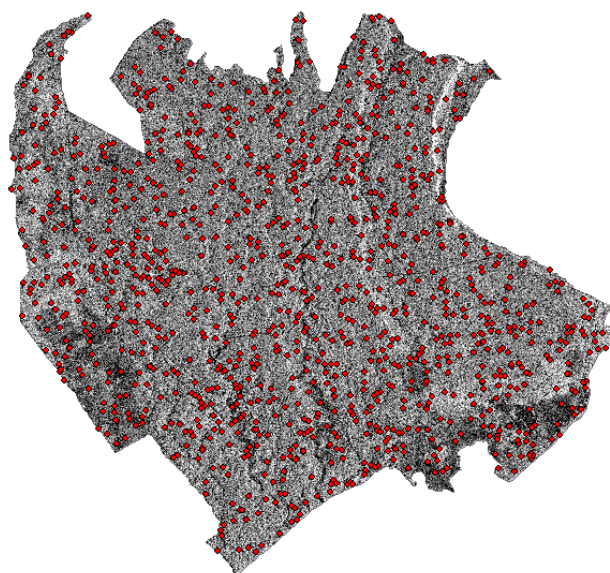
5.1. Correlation between the cross polarization

Backscatter image of HV and VH has been generated and the study area has been masked out from the Data. Figure 5-1 shows the regression analysis between the backscatter image of HV and VH. 1000 random points were generated randomly and correlation has been carried out between the backscatter images.



(a)

(b)



(c)

Figure 5-1: (a) Backscatter image of HV polarization, (b) Backscatter image of VH polarization,
(c) Random points for both HV and VH

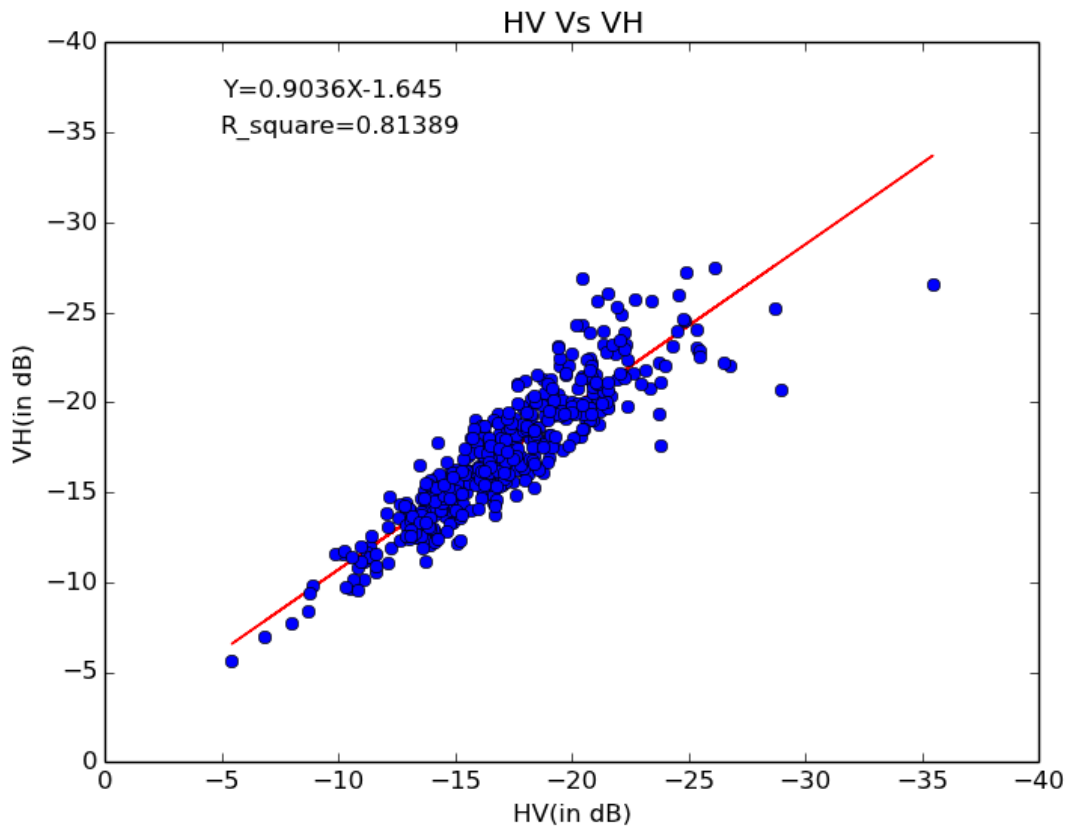


Figure 5-2: Linear regression analysis between HV and VH polarization.

Figure 5-2 shows the linear regression analysis between HV and VH polarization where the coefficient of determination known as R^2 is 0.81 which shows 81 percent of the value between the cross-pol channels is correlated.

5.2. Eigenvalue decomposition and results

Entropy parameter is extracted, using the H alpha decomposition, proposed by Cloude and Pottier from both the matrix i.e. T3 and T4.

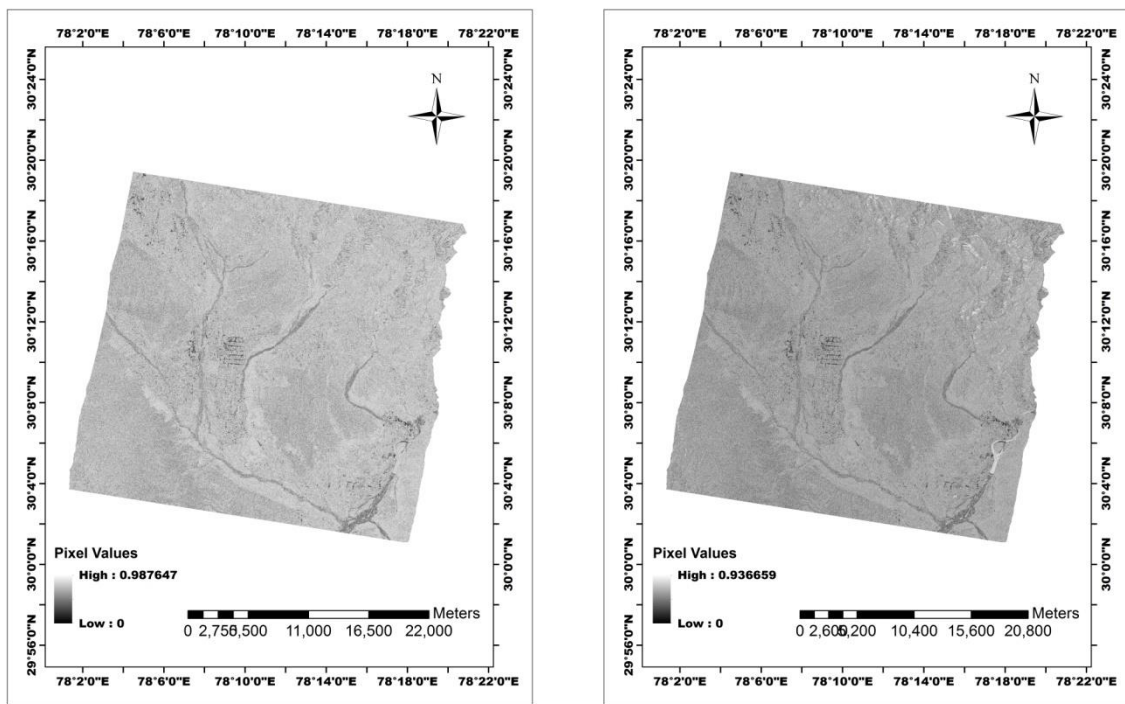
The values of entropy ranges from 0 to 1, the equation for entropy is given as

$$H = -\sum_{k=1}^N P_k \log_N(P_k) \quad (5.1)$$

Where P_i represents the probability obtained from the eigenvalues, N represents the dimension of the polarimetry (N=3 in the case of reciprocity and N=4 in the case of non-reciprocity).

For a weakly depolarizing system the entropy is generally low i.e. $H < 0.3$, where the scattering mechanism which is dominating can be easily identify. If the entropy value is high then there is no existence of equivalent point scatter. If the entropy is equal to 1 then the target scattering consist of random noise[43].

Entropy image generated from the coherency matrix decomposition under both reciprocity and Non reciprocity condition is shown in the Figure 5-3. Using the calculated biomass, the values of entropy is extracted for the particular field plot location. A linear regression model was applied on entropy and biomass in which 20 random points are chosen.

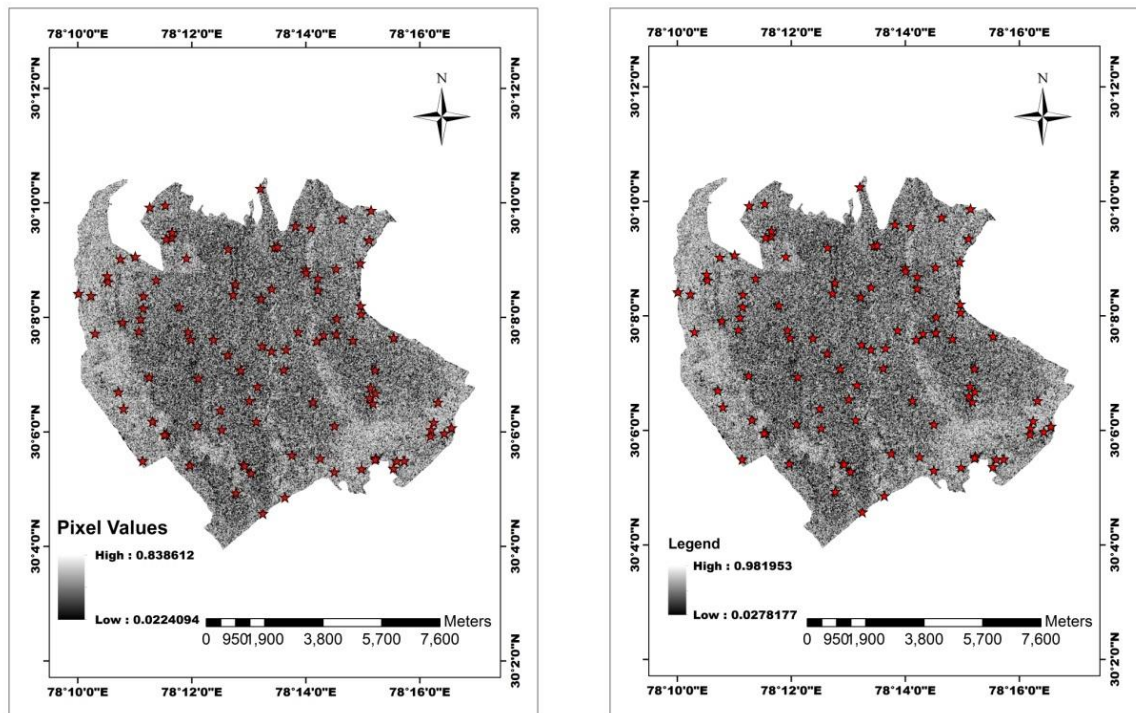


(a)

(b)

Figure 5-3: (a) Entropy image from T3 coherency matrix, (b) Entropy image from T4 coherency matrix

A plot which shows the variation for a sample of 100 points plotted from the study area responsible for Entropy from coherency matrix under reciprocity and non-reciprocity condition, shown in Figure 5-4. The line with blue colour shows the entropy for the coherency matrix under non reciprocity condition and the red line shows entropy from coherency matrix under reciprocity condition. It is visually visible from the graph that there is decrease in entropy under non-reciprocity condition that from the entropy from coherency matrix reciprocity



(a) (b)
Figure 5-4: (a) Entropy for T4 (b) Entropy for T3

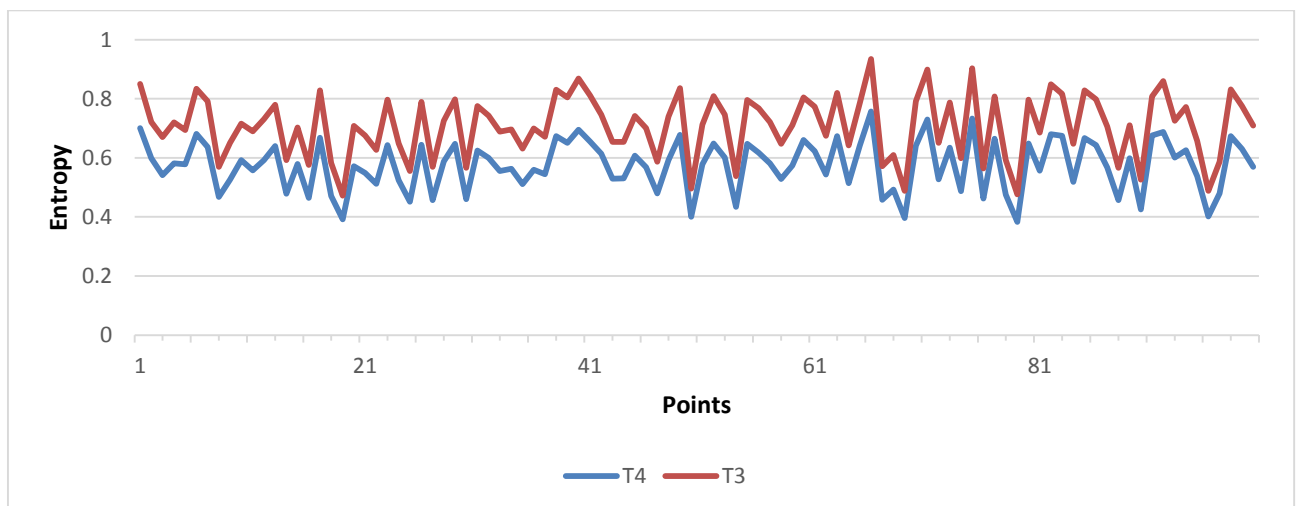


Figure 5-5: Entropy for T3 and T4

5.3. Regression Modelling for Biomass Estimation

Estimating the biomass is done using regression modelling. A sample of 17 points was taken from the field data and biomass was calculated. To train the data entropy values generated by decomposing the coherency matrix under reciprocity condition were extracted for the same plot

of sample points retrieved for field biomass. A linear regression analysis was done between the Entropy and biomass for the 17 sample points to obtain the correlation between them. Figure 5-6 shows linear regression model between the field biomass and the entropy, with R value of 0.50.

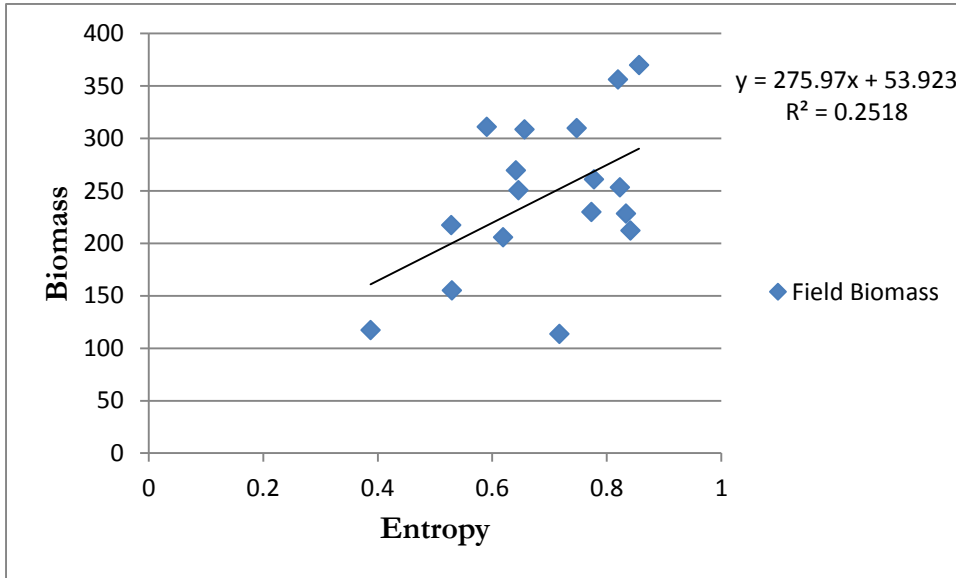


Figure 5-6: Regression analysis between Biomass and Entropy generated from the T3 coherency matrix

The above regression analysis shows there is 50% correlation between the sample point of field biomass and the entropy. Using the equation generated from the regression model, Biomass is calculated for the entropy generated from the decomposition of coherency matrix under non-reciprocity condition. A regression analysis was carried out between the estimated biomass from the field data to that of measured biomass using the above linear equation. Figure 5-7 shows the linear regression between the fields estimated and measured above ground biomass from both reciprocity and non-reciprocity condition.

RMSE is calculated for both the entropy from reciprocity and non-reciprocity condition with respect to the field measured above ground biomass, which is obtained by using

$$RMSE = \sqrt{\frac{\sum_{i=1}^N (AGB_{measured} - AGB_{estimated})^2}{N}} \quad (5.2)$$

Where, $AGB_{measured}$ is AGB obtain from field calculations, $AGB_{estimated}$ is the model estimated AGB and N is the number of plots used in modelling i.e. 28

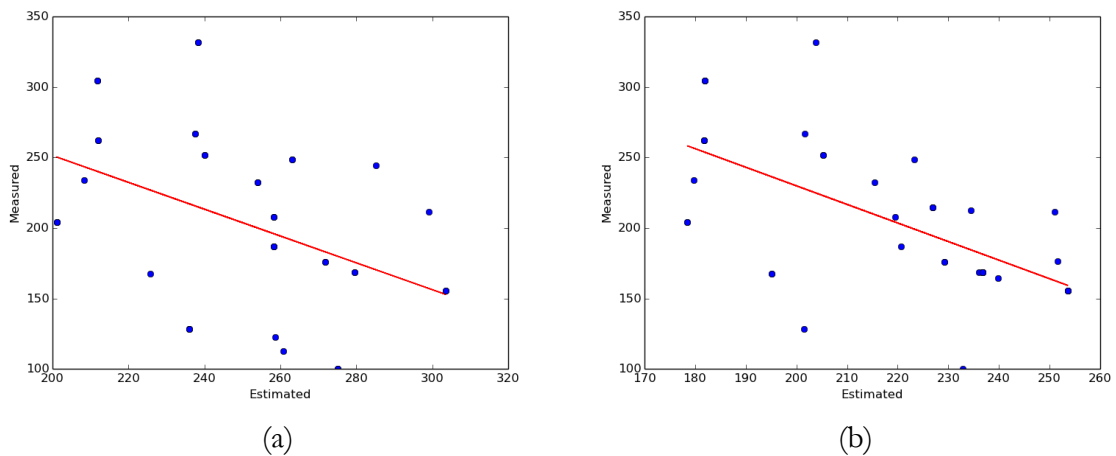


Figure 5-7: Regression Analysis over AGB for measure and estimated (a) Reciprocity (b) Non-Reciprocity

Table 5-1: RMSE and R-Square obtained from Modelled AGB under Reciprocity and Non-Reciprocity

Biomass	Reciprocity		Non-Reciprocity	
	RMSE (tons/ha)	R-Square	RMSE (tons/ha)	R-Square
	89.30519	0.183	68.50243	0.403

Table 5-1 shows the RMSE and the R-square calculated for the AGB obtained from the entropy decomposed from coherency matrix generated from both reciprocity and non-reciprocity condition. AGB obtained under non-reciprocity condition shows better RMSE and coefficient of determination (R-square).

5.4. DISCUSSION

The major focus of the research was to study how viable is the non-reciprocity symmetry suitable for retrieving upon the reciprocity using Radarsat 2 satellite c-band polarimetry data. C-band have

a wavelength of 5.5cm approximately and gives a scattering of forest canopy, not much penetrating trough canopy up to ground.

A 4×4 coherency matrix is retrieved under the concepts of non-reciprocity, where the cross polarized channel are meant to be not identical. Eigen decomposition was applied for both coherency matrix, i.e. under reciprocity and non-reciprocity condition. Using the eigenvalues of the coherency matrix, entropy is obtained using the eigen decomposition. In general, entropy values ranges from 0-1, if the entropy is low the, i.e. $H < 0$, describes that the point target is specifically identifiable where the system is having dominant scattering mechanism. If the entropy is high, i.e. $H = 1$, then the system is considered as a noise since it doesn't have a single equivalent point scatter.

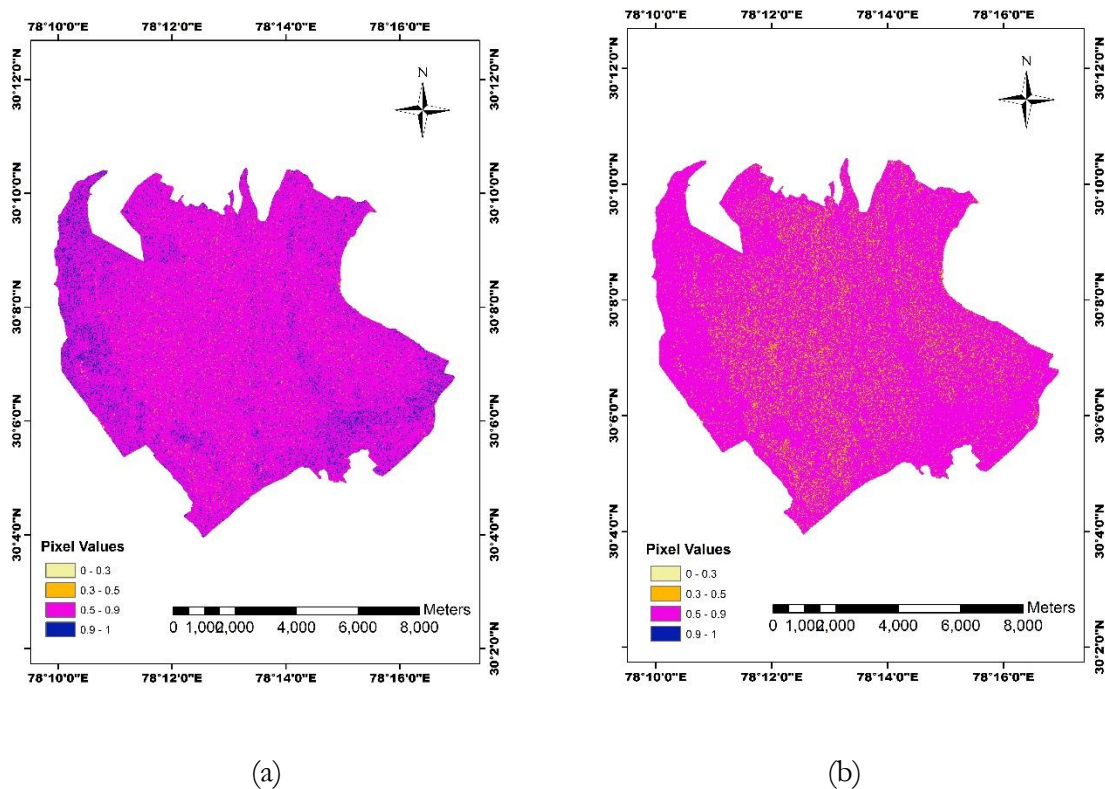


Figure 5-8: (a) Entropy under reciprocity, (b) Entropy under non-reciprocity

Figure 5-8 shows the entropy retrieved from eigen decomposition of coherency matrix of both reciprocity and non reciprocity condition, significantly the values from above 0.9 is considered as noise which is particularly viewed from the figure representing in blue of the entropy image under reciprocity condition where the entropy of non-reciprocity. Figure 5.5 also shows the line plot for the two entropy's achieved and also shows that entropy decreases for the coherency matrix under non-reciprocity that from the reciprocity condition.

The objective of the research was to achieve the forest biophysical parameter using the concepts of non reciprocity. The entropy achieved by Eigen decomposition of the coherency matrix helped to find the biophysical parameter using the regression modelling. Regression analysis over biomass and entropy from both the condition shows a promising the correlation of coefficient, though a negative correlation exists between them. The regression analysis was though done for 45 plots only which doesn't give effective concentration for the correlation between the biomass and the entropy.

6. CONCLUSION AND RECOMOMDATIONS

6.1. Conclusion

1) *Which technique can decompose a 4×4 coherency matrix?*

The research was concentrated on the techniques for decomposing the coherency matrix under non-reciprocity condition. Yamaguchi four decomposition model and Eigen decomposition by Cloudie concepts were used for the decomposition of coherency matrix. Using Eigen decomposition of the coherency matrix under non-reciprocity condition polarimetric scattering entropy was retrieved. Entropy defines the degree of randomness of the scattering process. It is a significant feature because it consider both the physical parameter, like biomass and canopy configuration, and also the randomness of the scattering media.

2) *Which scattering parameters will be needed for biomass estimation?*

The entropy H, defined by Eigen values of the coherency matrix, has significant feature because it consider both the physical parameter, like biomass and canopy configuration, and also the randomness of the scattering media.

3) *To what degree are non reflection symmetry based polarimetry parameters different from reflection symmetry based parameters?*

The research was focused in accessing the contribution of polarimetric scattering entropy from both reciprocity and non-reciprocity condition. Entropy values ranges from the 0-1, if the value is low then the point scatter obtained from the target can be specifically identified, and if the entropy is high i.e. if it tends to 1 then the system is considered as a noise since it doesn't have a single equivalent point scatter. Therefore, using Eigen decomposition technique entropy was obtained from both the coherency matrices, of which the entropy obtained from the 4×4 coherency matrix has less noise compared to the entropy from 3×3 coherency matrix.

4) *Can non reflection symmetry be used for retrieval of forest biophysical characteristics?*

Coherency matrix under non reciprocity condition is 4×4 positive hermitian matrix having real non-negative eigenvalues. The polarimetric scattering process of the terrain is shown by the amplitude and the difference of the four eigenvalues which are functionally associated to each other. Polarimetric scattering entropy, obtained from the Eigen decomposition of coherency matrix, is a significant feature because it consider both the physical parameter, like biomass and canopy configuration, and also the randomness of the scattering media. Consequently, Regression analysis was carried out between the entropy values and the biophysical parameters.

5) *How viable is the non reflection symmetry based polarimetry technique for estimating forest biophysical parameters in comparison to the results obtained by the field data?*

The correlation between the polarimetric scattering entropy, retrieved from coherency matrix under non-reciprocity condition, and the AGB is negative. Though the correlation is negative, the correlation of coefficient was found to be better than that of traditional method of reciprocity i.e. the r-squared value is 0.403 for the non-reciprocity case and 0.183 for reciprocity case. The RMSE also showed a slight variance, i.e. 68.50 for non-reciprocity and 89.30 for reciprocity case, which shows there is decrease of RMSE value describing that it is more effective than the reciprocity case.

6.2. Recommendations

The present research was focused on the decomposition of coherency matrix under non reciprocity condition where the cross polarized channels are meant to be not equal. The work was carried out using Eigen decomposition of coherency matrix. The following recommendations can be considered taking account the results obtained from this research.

- The present research was carried on the decomposition of coherency matrix using Eigen decomposition techniques. Other model based decomposition can also be used for the coherency matrix under non reciprocity condition like Yamaguchi and Freeman Durden decomposition to retrieve other scattering information.

- A semi-empirical model can also be used for the retrieval of biophysical parameters using a model based decomposition. Which can use other scattering information like Volume scattering information from the vegetation, scattering information from the surface and scattering information from the ground stem interaction. Which can possibly show a difference from the of coherency matrix under reciprocity condition.
- Research's has been done on deorientation on the coherency matrix under reciprocity condition, it will be difficult for apply the concepts of deorientaion on the coherency matrix under non reciprocity condition but the concepts can be done using scattering matrix.
- Present work was carried on the regression modelling, using 45 field samples of biomass which is consequently very less for analysis, the analysis can be more promising if more field data can be used which can be used in regression modelling which can give a better correlation between the polarimetric scattering entropy and the biomass.

REFERENCES

- [1] I. H. Woodhouse, *Introduction to microwave remote sensing*. Boca Raton: Taylor & Francis, 2006.
- [2] S. R. Cloude and E. Pottier, "A review of target decomposition theorems in radar polarimetry," *Geosci. Remote Sens. IEEE Trans. On*, vol. 34, no. 2, pp. 498–518, 1996.
- [3] H. A. Zebker and J. J. Van Zyl, "Imaging radar polarimetry: A review," *Proc. IEEE*, vol. 79, no. 11, pp. 1583–1606, 1991.
- [4] "Tutorial: Radar Polarimetry | Natural Resources Canada." [Online]. Available: <http://www.nrcan.gc.ca/earth-sciences/geomatics/satellite-imagery-air-photos/satellite-imagery-products/educational-resources/9579>. [Accessed: 08-Mar-2014].
- [5] S. Yin, P. B. Ruffin, and T. S. Francis, *Fiber optic sensors*, vol. 132. CRC Press LLC, 2008.
- [6] A. Shriniwas, "Polarimetric decomposition of SAR data for forest structure assessment," *Chalmers studentarbeten*, 2013. [Online]. Available: <http://studentarbeten.chalmers.se>. [Accessed: 08-Mar-2014].
- [7] Y. Yamaguchi, T. Moriyama, M. Ishido, and H. Yamada, "Four-component scattering model for polarimetric SAR image decomposition," *IEEE Trans. Geosci. Remote Sens.*, vol. 43, no. 8, pp. 1699–1706, Aug. 2005.
- [8] S.-W. Chen, X.-S. Wang, S.-P. Xiao, and M. Sato, "General Polarimetric Model-Based Decomposition for Coherency Matrix," *IEEE Trans. Geosci. Remote Sens.*, pp. 1–1, 2013.
- [9] J.-S. Lee and E. Pottier, *Polarimetric radar imaging: from basics to applications*. Boca Raton: CRC Press, 2009.
- [10] J. J. van Zyl, *Synthetic Aperture Radar Polarimetry*. John Wiley & Sons, 2011.
- [11] S. R. Cloude, *Polarisation*. Oxford; New York: Oxford University Press, 2010.
- [12] "Radar Polarimetry | Natural Resources Canada." [Online]. Available: <https://www.nrcan.gc.ca/earth-sciences/geomatics/satellite-imagery-air-photos/satellite-imagery-products/educational-resources/9275>. [Accessed: 25-Dec-2013].
- [13] W.-M. Boerner, W.-L. Yan, A.-Q. Xi, and Y. Yamaguchi, "Basic concepts of radar polarimetry," *Proc NATO Adv Res Work. Dir Inv Meth Radar Polar*, 1988.
- [14] W.-M. Boerner, H. Mott, and E. Luneburg, "Polarimetry in remote sensing: basic and applied concepts," in *Geoscience and Remote Sensing, 1997. IGARSS '97. Remote Sensing - A Scientific Vision for Sustainable Development., 1997 IEEE International*, 1997, vol. 3, pp. 1401–1403 vol.3.

- [15] S. R. Cloude and E. Pottier, "A review of target decomposition theorems in radar polarimetry," *Geosci. Remote Sens. IEEE Trans. On*, vol. 34, no. 2, pp. 498–518, 1996.
- [16] A. Freeman and S. L. Durden, "A three-component scattering model for polarimetric SAR data," *Geosci. Remote Sens. IEEE Trans. On*, vol. 36, no. 3, pp. 963–973, 1998.
- [17] F. Nunziata, M. Migliaccio, and C. E. Brown, "Reflection Symmetry for Polarimetric Observation of Man-Made Metallic Targets at Sea," *IEEE J. Ocean. Eng.*, vol. 37, no. 3, pp. 384–394, Jul. 2012.
- [18] S. H. Yueh, R. Kwok, and S. V. Nghiem, "Polarimetric scattering and emission properties of targets with reflection symmetry," *Radio Sci.*, vol. 29, no. 6, pp. 1409–1420, 1994.
- [19] E. Krogager, "New decomposition of the radar target scattering matrix," *Electron. Lett.*, vol. 26, no. 18, pp. 1525–1527, 1990.
- [20] Y. Yamaguchi, M. Ishido, H. Yamada, and T. Moriyama, "A Four-Component Decomposition of POLSAR Image," DTIC Document, 2005.
- [21] Y. Yamaguchi, Y. Yajima, and H. Yamada, "A four-component decomposition of POLSAR images based on the coherency matrix," *Geosci. Remote Sens. Lett. IEEE*, vol. 3, no. 3, pp. 292–296, 2006.
- [22] M. Sugimoto, K. Ouchi, and Y. Nakamura, "Four-Component Scattering Power Decomposition Algorithm with Rotation of Covariance Matrix Using ALOS-PALSAR Polarimetric Data," *Remote Sens.*, vol. 4, no. 12, pp. 2199–2209, Jul. 2012.
- [23] Y. Yamaguchi, T. Moriyama, M. Ishido, and H. Yamada, "Four-component scattering model for polarimetric SAR image decomposition," *IEEE Trans. Geosci. Remote Sens.*, vol. 43, no. 8, pp. 1699–1706, Aug. 2005.
- [24] S. R. Cloude and E. Pottier, "An entropy based classification scheme for land applications of polarimetric SAR," *Geosci. Remote Sens. IEEE Trans. On*, vol. 35, no. 1, pp. 68–78, 1997.
- [25] S. AGASHE, "Polarimetric Decomposition of SAR Data for Forest Structure Assessment."
- [26] B. Zou, P. He, H. Cai, and L. Zhang, "Target detection based on eigen-decomposition using PolInSAR data," in *2011 IEEE Radar Conference (RADAR)*, 2011, pp. 654–657.
- [27] K. U. Khan and Y. Jian, "Unsupervised Classification of Polarimetric SAR Images by Gamma-Correction of Features using Self Organizing Map," in *2007 International Symposium on Microwave, Antenna, Propagation and EMC Technologies for Wireless Communications*, 2007, pp. 1503–1507.
- [28] Y. Li, W. Hong, F. Cao, E. Chen, D. G. Goodenough, H. Chen, P. Wang, and A. Richardson, "Eigen decomposition parameter based forest mapping using Radarsat-2

- PolSAR data,” in *Geoscience and Remote Sensing Symposium (IGARSS), 2010 IEEE International*, 2010, pp. 4784–4787.
- [29] E. P. W. Attema and F. T. Ulaby, “Vegetation modeled as a water cloud,” *Radio Sci.*, vol. 13, no. 2, pp. 357–364, 1978.
- [30] M. Santoro, A. Shvidenko, I. McCallum, J. Askne, and C. Schmullius, “Properties of ERS-1/2 coherence in the Siberian boreal forest and implications for stem volume retrieval,” *Remote Sens. Environ.*, vol. 106, no. 2, pp. 154–172, Jan. 2007.
- [31] M. Santoro, C. Schmullius, J. Askne, and L. Eriksson, “Evaluation of JERS-1 L-band SAR backscatter for stem volume retrieval in boreal forest,” in *Geoscience and Remote Sensing Symposium, 2004. IGARSS '04. Proceedings. 2004 IEEE International*, 2004, vol. 1, pp. 515–518.
- [32] T. Mette, K. Papathanassiou, and I. Hajnsek, “Biomass estimation from polarimetric SAR interferometry over heterogeneous forest terrain,” in *Geoscience and Remote Sensing Symposium, 2004. IGARSS'04. Proceedings. 2004 IEEE International*, 2004, vol. 1, pp. 511–514.
- [33] Sanden D. H. Hoekman, “Radar remote sensing of tropical rain forests: the AIRSAR-93 campaign in Guyana and Colombia,” *Rapp. Iov Beleids Comm. Remote Sens. Delft 1996 59 Pp*, 1996.
- [34] M. C. Dobson, F. T. Ulaby, T. LeToan, A. Beaudoin, E. S. Kasischke, and N. Christensen, “Dependence of radar backscatter on coniferous forest biomass,” *IEEE Trans. Geosci. Remote Sens.*, vol. 30, no. 2, pp. 412–415, Mar. 1992.
- [35] T. Le Toan, A. Beaudoin, J. Riom, and D. Guyon, “Relating forest biomass to SAR data,” *IEEE Trans. Geosci. Remote Sens.*, vol. 30, no. 2, pp. 403–411, Mar. 1992.
- [36] K. J. Ranson and G. Sun, “Mapping biomass of a northern forest using multifrequency SAR data,” *IEEE Trans. Geosci. Remote Sens.*, vol. 32, no. 2, pp. 388–396, Mar. 1994.
- [37] H. ISRAELSSON, J. ASKNE, and R. SYLVANDER, “Potential of SAR for forest bole volume estimation,” *Int. J. Remote Sens.*, vol. 15, no. 14, pp. 2809–2826, Sep. 1994.
- [38] J. E. S. Fransson, “Estimation of stem volume in boreal forests using ERS-1 C- and JERS-1 L-band SAR data,” *Int. J. Remote Sens.*, vol. 20, no. 1, pp. 123–137, Jan. 1999.
- [39] T. M. Kuplich, V. Salvatori, and P. J. Curran, “JERS-1/SAR backscatter and its relationship with biomass of regenerating forests,” *Int. J. Remote Sens.*, vol. 21, no. 12, pp. 2513–2518, Jan. 2000.
- [40] C. S. A. Government of Canada, “RADARSAT-2,” *Canadian Space Agency website*, 12-Sep-2008. [Online]. Available: <http://www.asc-csa.gc.ca/eng/satellites/radarsat2/Default.asp>. [Accessed: 08-Mar-2014].

- [41] C. S. A. Government of Canada, "Satellite Characteristics," *Canadian Space Agency website*, 21-Jan-2011. [Online]. Available: <http://www.asc-csa.gc.ca/eng/satellites/radarsat/radarsat-tableau.asp>. [Accessed: 09-Mar-2014].
- [42] Y.-Q. Jin and F. Xu, *Polarimetric Scattering and SAR Information Retrieval*. John Wiley & Sons, 2013.
- [43] J.-S. Lee and E. Pottier, *Polarimetric radar imaging: from basics to applications*. Boca Raton: CRC Press, 2009.